

## Infrared Spectroscopy of Fragments of Protonated Peptides: Direct Evidence for Macrocyclic Structures of $b_5$ Ions

Undine Erlekam,<sup>‡</sup> Benjamin J. Bythell,<sup>†</sup> Debora Scuderi,<sup>‡</sup> Michael Van Stipdonk,<sup>§</sup>  
Béla Paizs,<sup>\*,†</sup> and Philippe Maître<sup>\*,‡</sup>

*Laboratoire de Chimie Physique, Université Paris-Sud 11, UMR8000 CNRS, Faculté des Sciences, Bât. 350, 91405 Orsay Cedex, France, Department of Chemistry, Wichita State University, Wichita, Kansas 67260, and German Cancer Research Center, Im Neuenheimer Feld 580, 69120 Heidelberg, Germany*

Received April 27, 2009; E-mail: Philippe.Maitre@u-psud.fr; B.Paizs@dkfz.de

**Abstract:**  $b$  ions are of fundamental importance in peptide sequencing using tandem mass spectrometry. These ions have generally been assumed to exist as protonated oxazolone derivatives. Recent work indicates that medium-sized  $b$  ions can rearrange by head-to-tail cyclization of the oxazolone structures generating macrocyclic protonated peptides as intermediates. Here, we show using infrared spectroscopy and density functional theory calculations that the  $b_5$  ion of protonated  $G_5R$  exists in the mass spectrometer as an amide oxygen protonated cyclic peptide rather than fleetingly as a transient intermediate. This assignment is supported by our DFT calculations which show this macrocyclic isomer to be energetically preferred over the open oxazolone form despite the entropic constraints the cyclic form introduces.

### Introduction

High-throughput protein identification and quantification in proteomics are primarily based on sequencing of proteolytic peptides by means of tandem mass spectrometry (MS/MS).<sup>1</sup> In these sequencing experiments, peptides are ionized by protonation, then introduced into the mass spectrometer where they undergo fragmentation following collisions with inert gas atoms/molecules (collision-induced dissociation (CID)). The resulting spectra usually contain sequence informative  $b$ ,  $a$ , and  $y$  peaks,<sup>2</sup> which are used to deduce the peptide sequences normally via the use of bioinformatics tools. These programs utilize fragmentation models<sup>3</sup> to generate theoretical spectra for candidate sequences, then measure the similarity between these theoretical spectra and the experimental MS/MS spectra. The sequence that best matches the experimental spectrum is then assigned. This strategy only performs well if the fragmentation model implemented predicts MS/MS spectra accurately. Regrettably, this is often not the case, so current sequencing software works with a high level of false positive identifications.<sup>4</sup> Utilizing more realistic fragmentation models should considerably improve the bioinformatics tools and, therefore, the accuracy of identifications of peptide sequence. Consequently, significant research effort is currently devoted to understanding the underlying

peptide fragmentation chemistry and the gas-phase structures responsible for it.<sup>5</sup>

The structure and reactivity of  $b$  ions has recently received significant attention. Most small  $b$  ions are thought to be truncated peptides terminated by the five-membered oxazolone ring at the C-terminus.<sup>6</sup> Experimental evidence supporting the oxazolone structure for small  $b_n$  ions was provided by CID studies,<sup>6,7</sup> gas-phase ‘action’ infrared spectroscopy,<sup>8</sup> H/D exchange,<sup>9</sup> and neutralization-reionization MS<sup>10</sup> studies on various  $b$  ions. The oxazolone structure is also supported by numerous computational studies.<sup>7d,8,10,11</sup> CID of small  $b_n$  ions usually results in the loss of CO to form the corresponding  $a_n$  ions which can then eliminate the C-terminal imine group to form the  $b_{n-1}$

<sup>‡</sup> Université Paris-Sud.

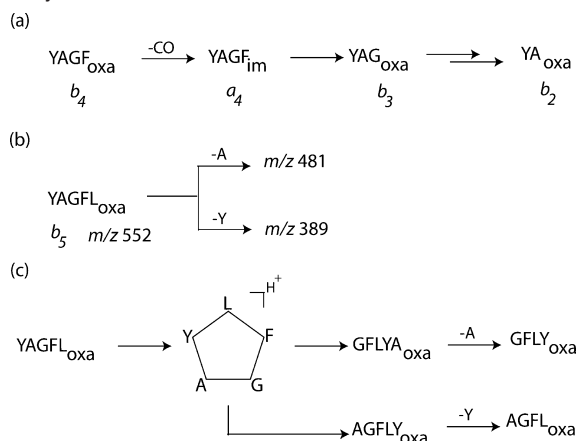
<sup>†</sup> German Cancer Research Center.

<sup>§</sup> Wichita State University.

- (1) (a) Aebersold, R.; Goodlett, D. R. *Chem. Rev.* **2001**, *101*, 269. (b) Steen, H.; Mann, M. *Nat. Rev. Mol. Cell Biol.* **2004**, *5*, 699.
- (2) (a) Roepstorff, P.; Fohlmann, J., *J. Biomed. Mass Spectrom.* **1984**, *11*, 601. (b) Biemann, K. *Biomed. Environ. Mass Spectrom.* **1988**, *16*, 99.
- (3) Paizs, B.; Suhai, S. *Mass Spectrom. Rev.* **2005**, *24*, 508.
- (4) (a) Taylor, G. K.; Goodlett, D. R. *Rapid Commun. Mass Spectrom.* **2005**, *19*, 3420. (b) Mol. Cell. Proteomics Home page: <http://www.mcponline.org>.

- (5) Paizs, B.; van Stipdonk, M. *J. Am. Soc. Mass Spectrom.* **2008**, *19*, 1717 and papers in this focus issue on peptide fragmentation.
- (6) (a) Yalcin, T.; Khouw, C.; Csizmadia, I. G.; Peterson, M. R.; Harrison, A. G. *J. Am. Soc. Mass Spectrom.* **1995**, *6*, 1165. (b) Yalcin, T.; Csizmadia, I. G.; Peterson, M. B.; Harrison, A. G. *J. Am. Soc. Mass Spectrom.* **1996**, *7*, 233. (c) Harrison, A. G. *Mass Spectrom. Rev.* **2009**, *28*, 640.
- (7) (a) Nold, M. J.; Wesdemiotis, C.; Yalcin, T.; Harrison, A. G. *Int. J. Mass Spectrom. Ion Processes* **1997**, *164*, 137. (b) Polce, M. J.; Ren, D.; Wesdemiotis, C. *J. Mass Spectrom.* **2000**, *35*, 1391. (c) Farrugia, J. M.; O’Hair, R. A. J.; Reid, G. E. *Int. J. Mass Spectrom.*, **2001**, *210–211*, 71. (d) Rodriguez, C. F.; Cunje, A.; Shoeib, T.; Chu, I. K.; Hopkinson, A. C.; Siu, K. W. M. *J. Am. Chem. Soc.* **2001**, *123*, 3006.
- (8) (a) Polfer, N. C.; Oomens, J.; Suhai, S.; Paizs, B. *J. Am. Chem. Soc.* **2005**, *127*, 17154. (b) Polfer, N. C.; Oomens, J.; Suhai, S.; Paizs, B. *J. Am. Chem. Soc.* **2007**, *129*, 5887. (c) Bythell, B. J.; Erlekam, U.; Paizs, B.; Maître, P. *J. ChemPhysChem* **2009**, *10*, 883. (d) Yoon, S. H.; Chamot-Rooke, J.; Perkins, B. R.; Hilderbrand, A. E.; Poutsma, J. C.; Wysocki, V. H. *J. Am. Chem. Soc.* **2008**, *130*, 17644. (e) Oomens, J.; Young, S.; Molesworth, S.; van Stipdonk, M. *J. Am. Soc. Mass Spectrom.* **2009**, *20*, 334.
- (9) (a) Reid, G. A.; Simpson, R. J.; O’Hair, R. A. J. *Int. J. Mass Spectrom.* **1999**, *190/191*, 209. (b) Bythell, B.; Somogyi, A.; Paizs, B. *J. Am. Soc. Mass Spectrom.* **2009**, *20*, 618. (c) Somogyi, A. *J. Am. Soc. Mass Spectrom.* **2008**, *19*, 1771.
- (10) Chen, X.; Turecek, F. *J. Am. Soc. Mass Spectrom.* **2005**, *16*, 1941.

**Scheme 1.** Summary of Fragmentation and Rearrangement Pathways of Small and Medium Sized  $b_n$  Ions<sup>a</sup>



<sup>a</sup> (a)  $b_4$  and  $b_3$  ions predominantly fragment by loss of CO and/or elimination of the C-terminal amino acid residue. This fragmentation behavior which gradually degrades  $b$  ions at their C-termini is accounted as ‘the oxazolone rule’. (b)  $b_5$  ions often fragment by eliminating internal or N-terminal amino acid residues.<sup>14</sup> (c) Elimination of non-C-terminal residues is explained by head-to-tail cyclization of the originally formed oxazolone (YAGFL<sub>oxa</sub>) to form the cyclic peptide isomer of the  $b_5$  ion. This then opens up at amide bonds other than the newly formed amide bond leading to oxazolones with scrambled amino acid sequence like GFLYA<sub>oxa</sub> and AGFLY<sub>oxa</sub>. The C-terminal amino acid residues of these sequences are eliminated according to ‘the oxazolone rule’. The subscripts ‘oxa’ and ‘im’ denote fragments with oxazolone and imine C-termini, respectively.

ion.<sup>6</sup> This stepwise degradation at the C-terminus, termed as ‘the oxazolone rule’ in the following, can be explained by the greater fragility of the C-terminal oxazolone group<sup>12</sup> compared to that of backbone amide bonds. In this way, small  $b$  ions usually fragment in an easily predictable manner as shown in Scheme 1a.

Conversely, there is increasing evidence to suggest that larger  $b$  ions may form macrocyclic structures which exhibit more complex fragmentation behavior. Boyd and co-workers<sup>13a,b</sup> demonstrated that  $b$  ions generated from Lys-containing peptides often eliminate internal, not C-terminal amino acid residues. The resulting peaks cannot be derived from the original peptide sequences based on ‘the oxazolone rule’, that is, on pathways that degrade the C-terminus. To account for these nontypical sequence ions, cyclization involving the Lys amine group and the then assumed C-terminal acylium,  $-C\equiv O^+$  group was proposed.<sup>13a,b</sup> Reopening of the macrocycle at amide bonds other than that from which it was formed leads to scrambled sequences

that can subsequently fragment to eliminate formerly internal amino acid residues. Later, Yague et al.<sup>13c</sup> showed that the same chemistry can be initiated by the N-terminal amine group as well.

Harrison and co-workers<sup>14a</sup> demonstrated that the fragmentation patterns from the  $b_5$  peak of YAGFL-NH<sub>2</sub> (formally YAGFL<sub>oxa</sub>, where the subscript ‘oxa’ refers to the oxazolone group at the C-terminus) and synthesized protonated cyclo-(YAGFL) are very similar and lead to elimination of the Y and A amino acid residues (Scheme 1b). Density functional calculations suggested<sup>14a</sup> that the YAGFL<sub>oxa</sub> isomer can undergo head-to-tail cyclization (associated barrier at  $\sim 17$  kcal mol<sup>-1</sup>) to form protonated cyclo-(YAGFL) (Scheme 1c). Since the initially formed oxazolone  $b$  ions are generated from parent peptide ions by crossing amide bond cleavage barriers ( $\geq 30$  kcal mol<sup>-1</sup>),<sup>3</sup> cyclization is energetically feasible. The cyclic peptide backbone can open up to form, for example, the AGFLY<sub>oxa</sub> and GFLYA<sub>oxa</sub> isomers which can then fragment further according to ‘the oxazolone rule’ by eliminating the C-terminal Y and A residues (Scheme 1c), respectively. A recent study<sup>14b</sup> demonstrated that cyclization of the original (oxazolone)  $b$  fragment and reopening of the macrocycle to form scrambled structures can be so pronounced that the original amino acid sequence cannot be derived from the CID spectra acquired for some  $b$  fragments, emphasizing the potentially critical role cyclic isomers play in the fragmentation chemistry of  $b$  ions. To distinguish between fragments arising directly from the original sequence and from scrambled sequences, a new nomenclature (*direct* versus *non-direct* sequence ions) was proposed.<sup>14a</sup>

Additionally, recent ion mobility spectroscopy (IMS) studies by Gaskell and co-workers<sup>15</sup> showed that the collision-cross sections of the  $b_5$  ion of YAGFL-NH<sub>2</sub> and protonated cyclo-(YAGFL) are very similar. Furthermore, low-energy CID of the  $b_5$  fragments<sup>14b</sup> derived from protonated YAGFL-NH<sub>2</sub>, AGFLY-NH<sub>2</sub>, GFLYA-NH<sub>2</sub>, FLYAG-NH<sub>2</sub>, and LYAGF-NH<sub>2</sub> leads to nearly identical product ion spectra. CID of the  $b_5$  fragment of protonated FLYAG-NH<sub>2</sub>,<sup>14b</sup> while producing abundant fragment ions, forms only minor direct sequence ions; i.e., it is not possible to recover the original amino acid sequence for the spectrum. These experimental findings were supported by a computational study of the potential energy surfaces (PESs) of protonated cyclo-(YAGFL) and the corresponding linear oxazolone-terminated isomers (YAGFL<sub>oxa</sub>, AGFLY<sub>oxa</sub>, GFLYA<sub>oxa</sub>, FLYAG<sub>oxa</sub>, and LYAGF<sub>oxa</sub>) which indicated<sup>14b</sup> that the most stable cyclic isomer is 6.9 kcal mol<sup>-1</sup> more so than any of the open forms. While these studies provided some useful insight into the structure and the cyclization-reopening chemistry of midsized  $b$  ions, no direct experimental evidence was available to support the existence of macrocyclic isomers of these ions, as opposed to their being transient intermediates in fragmentation reactions. Here, we investigate the structure of the  $b_5$  ion of protonated G<sub>5</sub>R by means of infrared multiple

- (11) (a) Paizs, B.; Lendvay, G.; Vékey, K.; Suhai, S. *Rapid Commun. Mass Spectrom.* **1999**, *13*, 525. (b) Paizs, B.; Suhai, S. *Rapid Commun. Mass Spectrom.* **2002**, *16*, 375. (c) Paizs, B.; Suhai, S. *J. Am. Soc. Mass Spectrom.* **2004**, *15*, 103. (d) Bythell, B. J.; Barofsky, D. F.; Pingitore, F.; Polce, M. J.; Wang, P.; Wesdemiotis, C.; Paizs, B. *J. Am. Soc. Mass Spectrom.* **2007**, *18*, 1291.
- (12) Allen, J. M.; Racine, A. H.; Berman, A. M.; Johnson, J. S.; Bythell, B. J.; Paizs, B.; Glish, G. L. *J. Am. Soc. Mass Spectrom.* **2008**, *19*, 1764.
- (13) (a) Tang, X.-J.; Thibault, P.; Boyd, R. K. *Anal. Chem.* **1993**, *65*, 2824. (b) Tang, X.-J.; Boyd, R. K. *Rapid Commun. Mass Spectrom.* **1994**, *8*, 678. (c) Yagüe, J.; Paradelo, A.; Ramos, M.; Ogueta, S.; Marina, A.; Barahona, F.; López de Castro, J. A.; Vázquez, J. *Anal. Chem.* **2003**, *75*, 1524.
- (14) (a) Harrison, A. G.; Young, A. B.; Bleiholder, B.; Suhai, S.; Paizs, B. *J. Am. Chem. Soc.* **2006**, *128*, 10364. (b) Bleiholder, C.; Osburn, S.; Williams, T. D.; Suhai, S.; Van Stipdonk, M.; Harrison, A. G.; Paizs, B. *J. Am. Chem. Soc.* **2008**, *130*, 17774. (c) Harrison, A. *J. Am. Soc. Mass Spectrom.* **2008**, *19*, 1776.

- (15) Riba-Garcia, I.; Giles, K.; Bateman, R. H.; Gaskell, S. J. *J. Am. Soc. Mass Spectrom.* **2008**, *19*, 609.
- (16) (a) Prazeres, R.; Glotin, F.; Insa, C.; Jaroszynski, D. A.; Ortega, J. M. *Eur. Phys. J. D* **1998**, *3*, 87. (b) MacAleese, L.; Simon, A.; McMahon, T. B.; Ortega, J. M.; Scuderi, D.; Lemaire, J.; Maitre, P. *Int. J. Mass. Spectrom.* **2006**, *249/250*, 14. (c) Lemaire, J.; Boissel, P.; Heninger, M.; Mauclair, G.; Bellec, G.; Mestdagh, H.; Simon, A.; Caer, S. L.; Ortega, J. M.; Glotin, F.; Maitre, P. *Phys. Rev. Lett.* **2002**, *89*, 27300.

photon dissociation (IRMPD) spectroscopy and density functional theory calculations.

## Experiments and Computations

**Mass Spectrometry and IR-MPD Spectroscopy.**  $G_5R$  (a gift from Á. Somogyi of University of Arizona, Tucson, AZ) was dissolved in  $CH_3OH/H_2O = 1:1$  with 2% acetic acid in a concentration range of 50–80  $\mu\text{mol}$  and was sprayed with conventional ESI conditions into a 3D quadrupole ion trap mass spectrometer (Bruker Esquire 3000+, Bremen, Germany). Helium was used as the collision gas. Following ionization,  $[G_5R + H]^+$  precursor ions were subjected to CID. The  $b_5$  peak was then mass-selected and subsequently subjected to IR irradiation. Upon resonant vibrational excitation, dissociation of the  $b_5$  ions into various fragments ( $b_5^\circ$ ,  $a_5$ ,  $a_5\text{-H}_2\text{O-NH}_3$ ,  $a_5^*$ ,  $b_4$ ,  $a_4$ ,  $a_4^*$ ,  $b_3$ ,  $b_3^\circ$ ,  $a_3^*$ , and  $b_2$ ) was observed. The abundances of these multiple fragment ions and  $b_5$  precursor ions were recorded as a function of the IR wavelength in order to derive the IR action spectra where the IRMPD efficiency<sup>16c</sup> is plotted against the photon energy. It should also be explicitly noted that the  $b_5$  peak of  $G_5R$  is *not* isobaric with any other likely reaction product, so represents an excellent medium-sized  $b$  ion model system.

Infrared spectroscopy was carried out using the free electron laser (FEL) at the Centre Laser Infrarouge d'Orsay (CLIO)<sup>16a</sup> coupled with the ion trap instrument. The details and performance of this experimental setup have been described previously.<sup>16b</sup> For the present experiment, the electron energy of the linear accelerator was set to 48 MeV, allowing the photon energy to be scanned from 1050 to 2050  $\text{cm}^{-1}$  by adjusting the undulator gap. The FEL power decreases as a function of undulator gap and, thus, of the photon energy. Consequently, additional scans were performed where the laser power was optimized in the 1800–2050  $\text{cm}^{-1}$  region. The combination of increased laser fluence and longer irradiation time (800 instead of 250 ms) was employed to confirm whether a diagnostic oxazolone C=O stretch peak was present. The IRMPD efficiency was corrected for the laser power variation.

**Computational and Theoretical Details.** A recently developed conformational search engine<sup>14a,b,17</sup> devised to deal with protonated peptides was used to scan the potential energy surfaces (PESs) of  $\text{GGGGG}_{\text{oxa}}$  and protonated cyclo-(GGGGG). These calculations began with molecular dynamics simulations using the Insight II program (Biosym Technologies, San Diego, CA) in conjunction with the AMBER force field, modified in-house in order to enable the study of structures with oxygen protonated amide bonds, protonated or neutral oxazolone groups, and amide bond cleavage transition structures (TS). During the dynamics calculations, we used simulated annealing techniques to produce candidate structures for further refinement, applying full geometry optimization using the modified AMBER force field.<sup>18</sup> These optimized structures were analyzed by a conformer family search program developed in Heidelberg. This program groups optimized structures into families in which the characteristic torsion angles of the molecule are similar. The most stable species in the families were then fully optimized at the PM3, HF/3-21G, B3LYP/6-31G(d), and finally at the B3LYP/6-31+G(d,p) level of theory. The conformer families were regenerated at each level and only structurally nondegenerate conformers were recomputed at the next level to prevent wasting computer time (i.e., only one of  $N$  identical structures is recomputed at the next level). This series of calculations was performed for the N-terminal amino and C-terminal oxazolone nitrogen protonated  $\text{GGGGG}_{\text{oxa}}$  and both amide oxygen and nitrogen protonated cyclo-(GGGGG) structures. Transition structures (TSs) for forming/

opening the macrocyclic isomer were probed in a similar fashion and all optimized structures were examined by vibrational analysis and then submitted to intrinsic reaction coordinate (IRC) calculations to determine which minima they connect. The total energies of the various optimized structures are presented in Table S1 (Supporting Information). Zero-point energy corrected relative energies were computed at the B3LYP/6-31+G(d,p) level. The Gaussian set of programs<sup>19</sup> was used for all *ab initio* and DFT calculations. Standard enthalpies, entropies, and free energies were calculated using the rigid-rotor harmonic oscillator (RRHO) approximation. In absolute terms, these are likely to be exaggerated due to the presence of too many low-frequency modes; however, relative enthalpies, entropies, and free energies are likely to be much more accurate due to cancellation of errors. Consequently, only relative terms are reported here. It should also be explicitly noted that the entropy values described herein refer to a situation of full thermodynamic equilibrium which is not necessarily the situation in our experiment. It is not our intention to claim this as being the case, merely to illustrate that such “entropic” considerations do not invalidate the conclusions reached in this manuscript.

The theoretical IR spectra were determined using harmonic frequencies scaled by a factor of 0.98 (the typical scaling factor in the spectral region explored here). The calculated stick spectra were convoluted assuming a Lorentzian profile with a 20  $\text{cm}^{-1}$  full width at half-maximum (fwhm). These are calculations performed within the harmonic approximation for single photon absorption and accordingly, using our method, one should expect some frequency deviations.<sup>20</sup> The experimental spectroscopic method employed here relies on the absorption of multiple photons, whereas the resulting IRMPD spectra are compared with single IR photon absorption spectra. While the multiple photon character of the spectrum can in principle make the IRMPD spectrum different from the calculated linear absorption spectra, studies on multiple molecular ions<sup>21</sup> show that the relative intensities and frequencies of the measured bands agree quite well with those predicted for linear IR absorption spectra by theoretical calculations. In comparison to one photon absorption spectra, a small red-shift in frequency has been observed, but this is only pronounced for strongly bound molecular ions. It should be stressed that the multiple photon absorption process occurs in an incoherent fashion, so that highly nonlinear power dependencies are unlikely. The IRMPD efficiency has also been shown to scale linearly with the FEL laser power,<sup>22</sup> which justifies the power correction employed in the present case.

The internal energy of the ions is an important factor influencing the line width of the observed IR bands. In the present experiments, the mass-selected  $b_5$  ions are expected to be thermalized by multiple collisions with the helium buffer gas, and a bandwidth on the order of 20  $\text{cm}^{-1}$  (fwhm) is expected.<sup>16b</sup>

## Results and Discussion

CID of singly protonated  $G_5R$  in the ion trap instrument results in sequence informative  $b$  and  $y$  ion peaks with significant abundances along with peaks resulting from small neutral losses (predominantly ammonia, for example,  $\gamma_4\text{-NH}_3$ ). An example spectrum is shown in Figure S1, Supporting Information. After isolation from the other CID peaks, the  $b_5$  ion undergoes fragmentation to form a number of product peaks. The exact

(17) (a) Wyttenbach, T.; Paizs, B.; Barran, P.; Brechi, L.; Liu, D.; Suhai, S.; Wysocki, V. H.; Bowers, M. T. *J. Am. Chem. Soc.* **2003**, *125*, 13768. (b) Paizs, B.; Suhai, S.; Hargittai, B.; Hruby, V. J.; Somogyi, A. *Int. J. Mass Spectrom.* **2002**, *219*, 203.  
(18) Case, D. A.; et al. *AMBER 99*; University of California: San Francisco, CA, 1999.

(19) Frisch, M. J.; et al. *Gaussian 03*; Gaussian, Inc.: Pittsburgh, PA, 2003.  
(20) Hall, M. D.; Velkovski, J.; Schlegel, H. B. *Theor. Chem. Acc.* **2001**, *105*, 413.

(21) Oomens, J.; Sartakov, B. G.; Meijer, G.; von Helden, G. *Int. J. Mass Spectrom.* **2006**, *254*, 1. (b) MacAleese, L.; Maître, P. *Mass Spectrom. Rev.* **2007**, *26*, 583. (c) Eyler, J. R. *Mass Spectrom. Rev.* **2009**, *28*, 448.

(22) (a) Simon, A.; MacAleese, L.; Maître, P.; Lemaire, J.; McMahon, T. B. *J. Am. Chem. Soc.* **2007**, *129*, 2829. (b) Bakker, J. M.; Besson, T.; Lemaire, J.; Scuderi, D.; Maître, P. *J. Phys. Chem. A*, **2007**, *111*, 13415.



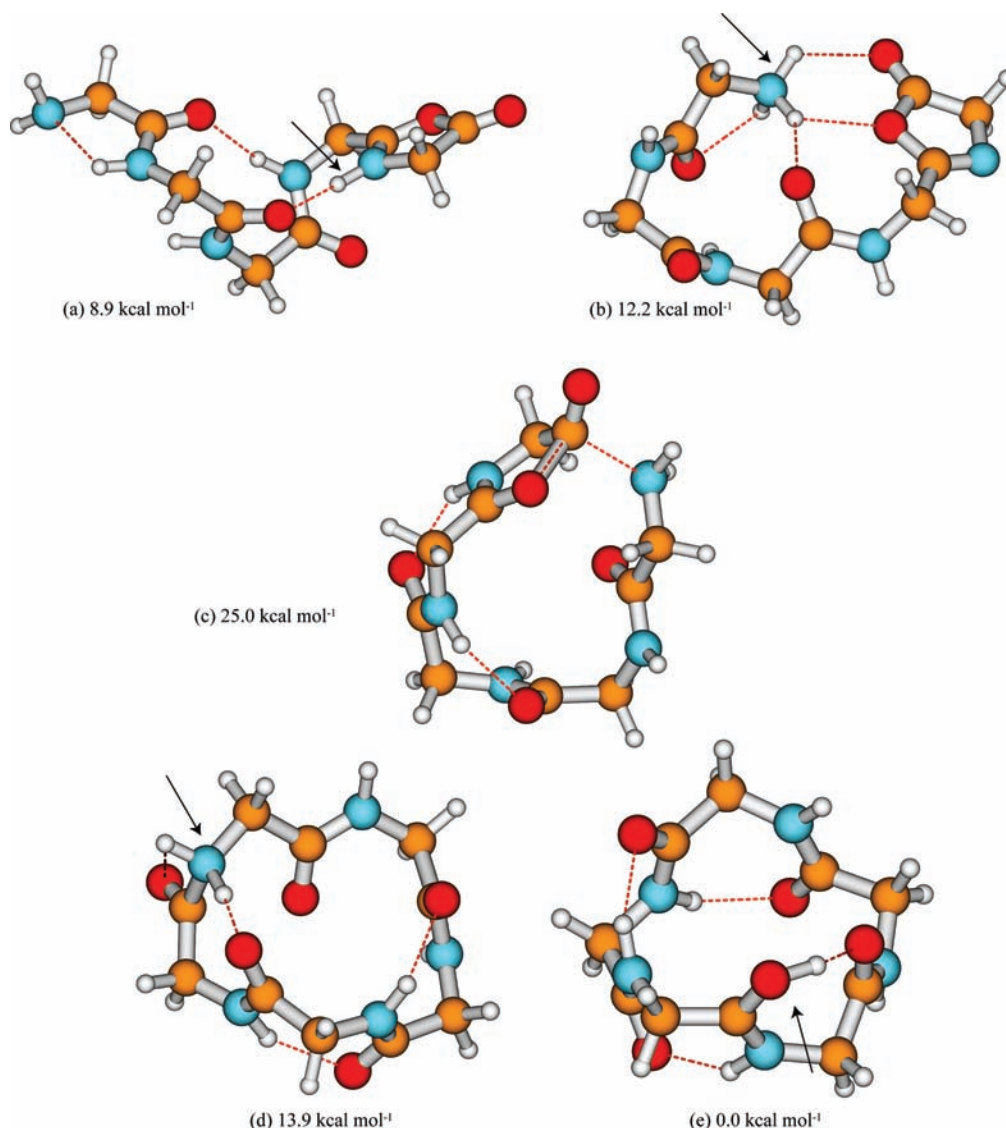


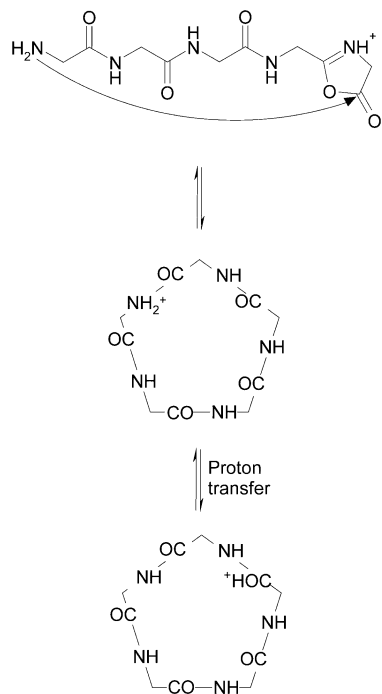
**Figure 1.** Selected structures on the PES of  $b_5$  from protonated  $G_5R$ . (a) Oxazolone ring nitrogen protonated form; (b) N-terminal amino protonated oxazolone form; (c) transition structure on the cyclization/ring-opening pathway; (d) macrocyclic isomer protonated at an amide nitrogen; (e) macrocyclic isomer protonated at an amide oxygen. Relative energies determined at the B3LYP/6-31+G(d,p) level of theory are given for clarity. An arrow indicates the site of protonation in each case.

peaks and relative intensities vary as a function of the excitation amplitude, for example,  $b_5^\circ$ ,  $a_5$ ,  $b_5^{\circ*}$ ,  $a_5^*$ ,  $a_5^*-\text{CO}$ ,  $b_3$ , and  $b_2$  were formed in the CID spectrum shown in Figure S2 (Supporting Information). This CID fragmentation pattern is compatible with either or both of the  $\text{GGGGG}_{\text{oxa}}$  and protonated cyclo-(GGGGG)  $b_5$  structures, so in this case the CID experiments do not provide any structural information on the  $b_5$  ions being fragmented.

Cleavage of the G-R amide bond of protonated  $G_5R$  leads to formation of the oxazolone  $b_5$  isomer or the  $y_1$  ion (Figure S1).<sup>3</sup> The  $b_5$  oxazolone structure has two competitive protonation sites: the oxazolone ring and the N-terminal amino nitrogens (Figure 1, panels a and b, respectively.) Both forms are stabilized by strong H-bonds which effectively shield the ionizing charge. Our calculations indicate (Table S1, (Supporting Information)) that protonation at the oxazolone nitrogen (Figure 1a) is 3.3 kcal mol<sup>-1</sup> more energetically favored than protonation at the N-terminus (Figure 1b). The oxazolone protonated form can undergo head-to-tail cyclization (Scheme 2; TS is shown in Figure 1c) by nucleophilic attack of the N-terminal amino

nitrogen on the carbonyl carbon of the N-protonated oxazolone ring.<sup>14</sup> The barrier to this reaction is 16.1 kcal mol<sup>-1</sup> relative to the oxazolone protonated isomer, which is in good agreement with the results from prior work on the  $b_5$  ions with YAGFL permuted sequences.<sup>14b</sup>

The resulting macrocyclic structures are protonated at an amide nitrogen (Scheme 2 and Figure 1d), but then undergo rapid intramolecular proton transfer (negligible barrier) to form the energetically more stable amide oxygen protonated forms (Scheme 2 and Figure 1e). Five such amide oxygens are available for  $b_5$  ions as competing protonation sites which are equienergetic for the  $b_5$  ion derived from  $[G_5R + H]^+$ . Our calculations indicate that the amide oxygen protonated cyclic form is 8.9 kcal mol<sup>-1</sup> more energetically favored than the most favorable oxazolone isomer. Correction for the entropic constraints placed upon the  $b_5$  ion by forming a cyclic structure as calculated based on the rigid-rotor harmonic oscillator (RRHO) approximation leads to a  $\Delta G_{298}$  of 6.4 kcal mol<sup>-1</sup> with a corresponding  $\Delta S_{298}$  of 11.8 cal K<sup>-1</sup> mol<sup>-1</sup> (Table S1). This indicates that the linear oxazolone form is still significantly less stable than the cyclic

**Scheme 2.** Head-to-Tail Cyclization of the Oxazolone Nitrogen Protonated Linear  $b_5$  Isomer from Protonated  $G_5R^a$ 


<sup>a</sup> This reaction forms an amide nitrogen protonated intermediate that undergoes rapid proton transfer resulting in the energetically more stable amide oxygen protonated form.

isomer. Additionally, it should be noted here that the RRHO entropy correction does not contain the terms that arise due to the existence of energetically degenerate or quasidegenerate isomers. Considering such ‘conformational’ entropy terms would likely favor the cyclic form even more here as five equienergetic structures exist, whereas the linear forms only have a couple of quasidegenerate structures for which to account. Obviously, this effect is likely to be lessened somewhat for  $b_5$  ions containing differing amino acids where the degeneracy of the cyclic form will be decreased.

To investigate whether linear oxazolone or macrocyclic  $b_5$  ions are present in the mass spectrometer, IRMPD experiments were carried out in the mid-IR range ( $1050\text{--}2050\text{ cm}^{-1}$ ) to probe the C=O stretch and C–O–H bending modes which facilitate characterization of the oxazolone and cyclic peptide  $b_5$  isomers. The resulting experimental spectrum with theoretical spectra computed for the most likely isomers and protonation sites of each type are shown in Figure 2. The corresponding structures and energies are shown in Figure 1 and Table S1 (Supporting Information), respectively. To assign our experimental IRMPD spectrum, one has to consider the theoretical spectra for the energetically most favored amide oxygen protonated macrocyclic structure (Figure 1e), along with the N-terminal amino and ring nitrogen protonated oxazolone forms (Figure 1, panels a and b). The calculated cyclic peptide and oxazolone spectra of the  $b_5$  ion of  $[G_5R + H]^+$  differ substantially and feature structure specific motifs (Figure 2). The range between  $1800$  and  $2000\text{ cm}^{-1}$  is the most diagnostically useful part of the IRMPD spectrum. Here, each oxazolone isomer has a strongly active IR band associated with the lactone C=O stretch. Our calculations indicate that the C=O frequency is  $\sim 1945\text{ cm}^{-1}$  for the oxazolone ring nitrogen protonated structures, whereas it is red-shifted to  $\sim 1830\text{ cm}^{-1}$  when the lactone is involved in hydrogen bonds with the protonated

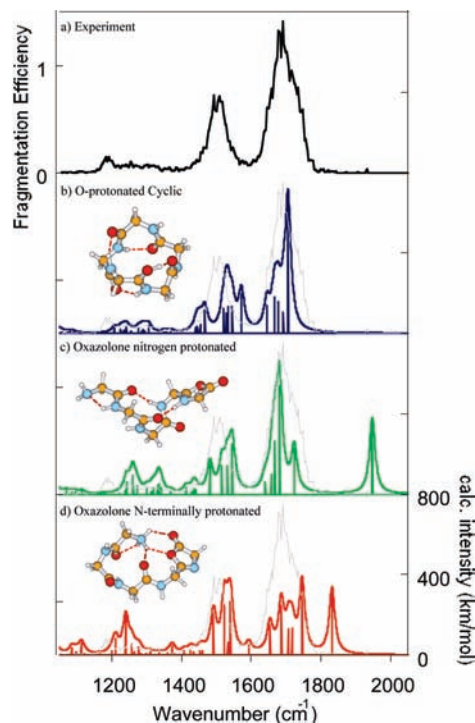


**Figure 2.** Infrared spectra of the  $b_5$  ion of protonated  $G_5R$ . (a) Experimental IRMPD spectrum; (b) calculated spectrum (blue) of the O-protonated cyclic isomer overlaid on the experimental (gray) spectrum; (c) the calculated (green) oxazolone ring protonated isomer overlaid on the experimental (gray) spectrum; and (d) the calculated (red) oxazolone N-terminally protonated isomer overlaid on the experimental (gray) spectrum.

N-terminus, where the positive charge has been removed from the ring nitrogen (Figure 2, panels c and d, respectively). Prior work on  $b_2$  and  $b_4$  ions clearly demonstrated absorption at similar wavenumbers for oxazolone structures.<sup>8</sup> Experimentally, however, no significant peak is observed here for the  $b_5$  ion of  $[G_5R + H]^+$ . Additional scans where the laser power was optimized to the  $1800\text{--}2050\text{ cm}^{-1}$  region were performed with longer irradiation time (800 instead of 250 ms) to confirm that no oxazolone C=O stretch peak could be detected. In contrast, the cyclic peptide theoretical spectrum (Figure 2b) is much more similar to the experimental spectrum over the whole spectral range explored here than those calculated for the oxazolone structures. The two main experimental features centered at  $\sim 1500$  and  $\sim 1700\text{ cm}^{-1}$  are only slightly red-shifted as compared to the two maxima in the theoretical spectrum of the O-protonated macrocyclic isomer. This strongly supports the O-protonated macrocyclic isomer as being the form of the  $b_5$  ion present in the mass spectrometer.

It is also important to note that fragmentation of the oxazolone isomer is clearly *less* energetically demanding than dissociation of the macrocyclic isomer, as the former does not require proton transfer reactions to an amide nitrogen to initiate fragmentation. This is due to the fact that the oxazolone isomers initially fragment by eliminating CO or water<sup>3,6,12,14,23</sup> directly, but such reactions are not likely for the O-protonated cyclic structure. Instead, proton transfer to an amide nitrogen occurs first, followed by opening of the macro-ring,<sup>3,14</sup> to form oxazolone isomers (reaction cascade in Scheme 1 from bottom to top) which then undergo the dissociations monitored when acquiring

(23) Paizs, B.; Szlávik, Z.; Lendvay, G.; Vékey, K.; Suhai, S. *Rapid Commun. Mass Spectrom.* **2000**, *14*, 746.

IRMPD spectra. In effect, an additional  $\sim 9$  kcal mol<sup>-1</sup> is needed to fragment the macrocyclic structures. This means that the current excitation method, which uses absorption of multiple photons at a given wavenumber to induce fragmentation, should be *more* sensitive to the presence of oxazolone isomers than to the cyclic peptide forms. Despite this, no significant absorption is observed at the oxazolone specific frequencies, which suggests that the  $b_5$  ion population contains solely cyclic isomers. This experimental and computational evidence clearly contradicts the generally accepted view that cyclization reactions are favored only for smaller ring-size (mostly to form 5- and 6-membered rings). Here, we have evidence for the gas-phase formation and gas-phase stability of a 15-membered ring.

There is no evidence of oxazolone ring protonated  $b_5$  ions in Figure 2. However, there are a couple of very small absorption peaks in the IRMPD spectrum, blue-shifted from the edge of the large backbone C=O stretch peak which ends at  $\sim 1800$  cm<sup>-1</sup>. Despite the preceding energetic and mechanistic argument, we cannot completely exclude the possibility of these corresponding to a very small population of N-terminally protonated oxazolone  $b_5$  ions being present in the mass spectrometer too.

### Conclusions

Recent CID studies on medium-sized  $b$  ions indicate that cyclic peptide isomers do play an important role in the dissociation of these sequence ions.<sup>14</sup> However, no direct experimental evidence to confirm the existence of such  $b$  ions as stable species, rather than fleeting transient intermediates, has been available until now. Our combined infrared spectroscopy and theoretical study provides direct evidence that the  $b_5$  ion of  $[G_5R + H]^+$  has a macrocyclic structure under the experimental conditions applied. Consequently, other medium-

sized  $b_n$  ions ( $n \geq 5$ ) are likely to exist in ion trap mass spectrometers as macrocyclic structures. This experimental discovery goes against the conventional wisdom that such large cyclic structures should not be populated due to entropic constraints. This finding is supported by our DFT calculations which show this macrocyclic isomer to be energetically preferred over the open oxazolone form despite the entropic constraints the cyclic form introduces.

The existence of these macrocyclic, medium-sized  $b_n$  ions (or larger ones) is an obvious potential impediment if these ions subsequently fragment as proposed elsewhere,<sup>14</sup> as this can produce *nondirect* or 'scrambled' sequence ions. If this is the case, then these 'sequence scrambling' fragmentations of such large macrocyclic ions need to be considered when analyzing MS/MS spectra. At present, none of the data processing strategies in proteomics incorporate this possibility into their code, thereby increasing the rate of false peptide and protein identifications.

**Acknowledgment.** The authors thank A. Somogyi for providing the G<sub>5</sub>R peptide. B.J.B. thanks the DKFZ for a guest scientist fellowship. Financial support by the European Commission EPITOPES project (NEST program, project #15367) is gratefully acknowledged. The authors are grateful to J. M. Ortega, J. P. Berthet, C. Six, G. Perilhous, J. Lemaire, and E. Nicol for technical support.

**Supporting Information Available:** Total energies of the species presented in the text, CID spectra of protonated G<sub>5</sub>R and its  $b_5$  ion, and complete refs 18 and 19. This material is available free of charge via the Internet at <http://pubs.acs.org>.

JA903390R